NMR Spectroscopy of MOFs

DOI: 10.1002/ange.201106030

Dynamic Nuclear Polarization Enhanced Solid-State NMR Spectroscopy of Functionalized Metal–Organic Frameworks**

Aaron J. Rossini, Alexandre Zagdoun, Moreno Lelli, Jérôme Canivet, Sonia Aguado, Olivier Ouari, Paul Tordo, Melanie Rosay, Werner E. Maas, Christophe Copéret, David Farrusseng, Lyndon Emsley, and Anne Lesage**

Metal–organic frameworks (MOF) constitute an important class of crystalline porous materials.[1] Since the introduction of the first porous MOF more than twenty years ago,[2] more than 2000 three-dimensional MOF topologies have been described. The large surface areas (up to 6000 $m^2 g^{-1}$) and tunable pore sizes (ranging from 0.5 to 3 nm) of MOFs makes them well suited for a variety of applications including gas storage, molecular sieving, or heterogeneous catalysis.[3] Many MOF materials have been shown to be efficient and selective catalysts in a wide variety of key chemical reactions. As for other classes of solid catalysts, establishing structure–activity relationships is key for the rational design of MOFs with improved catalytic properties.

Solid-state nuclear magnetic resonance (NMR) spectroscopy is well suited to characterize the molecular structure and dynamics of MOF materials, for example in cases where X-ray diffraction is insufficient to determine the topology of the framework[3b,c,4] or when the flexibility properties of the network needs to be investigated.[6]

We have recently shown how dynamic nuclear polarization[7] (DNP) could be implemented to yield a remarkable increase in the NMR sensitivity for surface organic functionalities in hybrid nanoporous materials.[8] The drastic reduction in experiment time (of more than two orders of magnitude) provided by DNP ^{13}C or ^{29}Si solid-state NMR spectroscopy allowed the fast and detailed structural characterization of surface bonding patterns and local conformations.[11]

We report here the first application of DNP-enhanced solid-state NMR spectroscopy to MOF materials. The experiments are demonstrated on the N-functionalized MOF compound (In)-MIL-68-NH_2[4,12,13] (**1**), on a partially functionalized variant of **1** with a terephthalate:aminoterephthalate ratio of 80:20 (**2**), and on a 10% proline-functionalized derivative of **1**,[14] (In)-MIL-68-NH-Pro (**3**) (Scheme 1). These three materials are representatives of an as-synthesized functionalized MOF (compound **1**), a partially functionalized MOF (also called MIXMOF,[15] compound **2**), and of a post-synthetically modified MOF (compound **3**).[16] Despite the fact that the pore size of the MOFs are much smaller (ca. 1.6 nm) than that of the mesoporous materials we previously investigated by DNP surface-enhanced solid-state NMR (ca. 6 nm),[8,11] we show that significant effective sensitivity enhancement factors can be obtained for ^1H-^{13}C cross-polarization magic angle spinning (CPMAS) experiments on these MOF materials. These factors are discussed with respect to the presence or not of the bulky proline ligand, which prevents the radical from entering into the pores. We show in addition that the reduction in experimental time provided by the DNP technology (of the order of 10- to 30-fold) allows the fast acquisition of two-dimensional ^1H-^{13}C correlation spectra and of ^1H-^{15}N CPMAS NMR spectra at natural abundance.

Figure 1 A, B and C shows the one-dimensional ^1H-^{13}C CPMAS spectra recorded on the three MOF samples with or without microwave (MW) irradiation to induce DNP. The observed DNP enhancement (ε) and the overall sensitivity enhancement factors (Σ) are indicated for each of the three compounds. While ε is defined as the ratio of the signal-to-noise ratio of the MW on and MW off spectra, Σ corresponds to the sensitivity gain with respect to a dry sample at low temperature. The definitions of the various sensitivity enhancement factors are given in the Supporting Information and have previously been extensively discussed.[17] Notably, Σ takes into account the fact that the signal enhancement available from DNP is partially offset due to reductions in signal intensities by various paramagnetic effects.

We have recently presented a series of non-aqueous solvents that, in combination with the exogenous biradical bTbK[5] yield enhancements comparable to the best available water-based systems.[18] As the MOF samples investigated

[*] Dr. A. J. Rossini, A. Zagdoun, Dr. M. Lelli, Prof. L. Emsley, Dr. A. Lesage
Centre de RMN à Très Hauts Champs
Université de Lyon (CNRS/ENS Lyon/UCB Lyon 1)
5, rue de la Doua, 69100 Villeurbanne (France)
E-mail: lyndon.emsley@ens-lyon.fr
anne.lesage@ens-lyon.fr
Homepage: http://crmn.ens-lyon.fr
Dr. J. Canivet, Dr. S. Aguado, Dr. D. Farrusseng
Institut de Recherche sur la Calayse et l'Environnement de Lyon (IRCELYON)
Université de Lyon (CNRS), 69626 Villeurbanne (France)
Prof. C. Copéret
Department of Chemistry, ETH Zürich, Laboratory of Inorganic Chemistry, 8093 Zürich (Switzerland)
Dr. O. Ouari, Prof. P. Tordo
SREP LCP UMR 6264, Faculte de Saint Jerome case 521
13013 Marseille (France)
Dr. M. Rosay, Dr. W. E. Maas
Bruker BioSpin Corporation, Billerica, MA 01821 (USA)

[**] A.J.R. acknowledges support from a EU Marie-Curie IIF Fellowship (PIIF-GA-2010-274574). Financial support is acknowledged from EQUIPEX contract ANR-10-EQPX-47-01, and the ETH Zürich.

Supporting information for this article (complete experimental details) is available on the WWW under http://dx.doi.org/10.1002/anie.201106030.

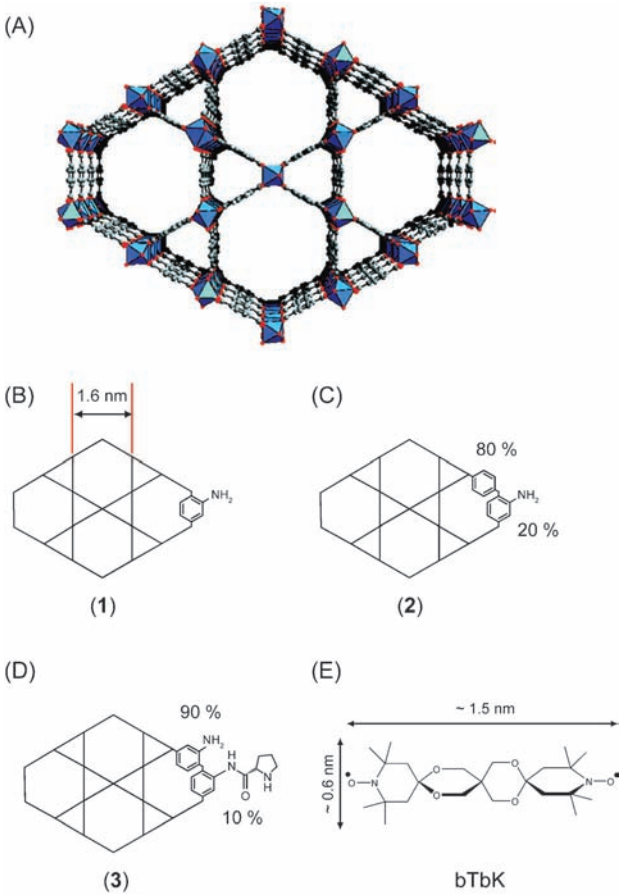

Scheme 1. A) The crystal structure of MOF (In)-MIL-68 illustrating the three-dimensional structures of the MOFs that are formed with indium octahedra and terephthalate ligands as bridging linkers.[4] B–D) Schematic structures of the three N-functionalized MOFs which are isostructural to MIL-68. B) (In)-MIL-68-NH_2 (**1**), C) the partially N-functionalized (In)-MIL-68 material obtained with a terephthalate:2-aminoterephthalate ratio of 80:20 (**2**), and D) the 10% proline-functionalized derivative of (**1**), (In)-MIL-68-NH-Pro (**3**). All MOFs display one-dimensional rod-shaped structures, composed by hexahedral and triangular channels with an aperture of 1.6 and 0.6 nm, respectively. E) Schematic structure of the biradical polarizing agent bTbK.[5] The approximate size of the molecule is 1.5 nm × 0.6 nm.

here could not be impregnated with an aqueous solution (due to a chemical reaction with water), solutions of the biradical bTbK (Scheme 1)[5] and 1,1,2,2-tetrachloroethane ($EtCl_4$) were utilized. Incipient wetness impregnation was used to impregnate the dry materials with a minimal amount of radical containing solution. All details about sample preparation and optimization of the experimental conditions are given in the Supporting Information. In particular the influence of radical concentration, spinning frequency (ν_{rot}), and the amount of time the impregnated samples were allowed to rest before solid-state NMR experiments were attempted, were optimized on **1**.

It was found that 16 mM bTbK solutions provided both the highest ε and Σ (Supporting Information, Figure S1). Although ε was observed to be higher with a sample spinning frequency ν_{rot} of 8 kHz, the absolute signal of the spectra was similar with a ν_{rot} of 12 kHz (Figure S2). In order to reduce overlap of spinning sidebands with isotropic resonances, a ν_{rot} of 12 kHz was employed for all subsequent experiments. Finally, DNP ^{1}H-^{13}C CPMAS solid-state NMR spectra of the same sample of **1** impregnated with a 16 mM bTbK solution were periodically acquired after the sample was allowed to rest on the bench top inside the rotor for times of 5 min, 1 h and 25 h in between acquisitions. Both ε and Σ were observed to steadily increase from 7 to 13 and 3.0 to 3.6, respectively, with longer sample resting times (Figure S3). This suggests the biradical species slowly diffuse through the relatively small (1.6 nm) pores of the material. Spectra of **1** and **2** were recorded after 25 and 0.5 h of resting time, respectively. For compound **3**, however, the enhancement factors were independent of sample resting time and spectra were recorded 5 min after rotor packing. Note that the enhancements for the $EtCl_4$ resonance ($\varepsilon_S > 20$ in all cases) is always larger than that for the MOF materials, suggesting that the biradical molecules are partly excluded from the pores for all three types of the materials (see below).[19]

Under these optimal experimental conditions, for MOF samples **1** and **2**, ε values of 13 and 16 were observed, respectively. Significantly lower values of Σ were measured, corresponding to the fact that the biradicals inside of the material cause a reduction in the signal intensity through various paramagnetic effects.[17] On the other hand, for **3**, similar values of ε and Σ are observed (4.8 and 5.8, respectively). This strongly suggests that the bTbK molecules are excluded from the pores of **3**, leading to a low value for ε, and a relatively high value for Σ. This suggests that the whole material is contributing to the NMR signal under DNP conditions. This is in agreement with the fact that for **3**, ε does not increase with additional sample resting times, and that a much larger value of ε is observed for the solvent resonances ($\varepsilon_S = 26$). It is likely that for **3**, the proline groups block the one-dimensional pores of the material and hinder the relatively large bTbK radical from diffusing into the material. TEM images of the as prepared **3** reveal that the average crystal size is less than 300 nm (Figure S4). Griffin and coworkers have previously applied DNP to needle-like nanocrystalline peptides which possessed an average crystal width of 150 nm.[19] In their system it was not possible for the radical to enter the lattice of the crystal and larger ε values were obtained for the solvent resonances than the resonances of nuclei inside the crystals, as observed here. In a similar way, we postulate that for **3**, the bTbK molecules reside on or near the surface of the crystallites, and that the enhanced polarization is distributed into the crystal by spin diffusion.

For all three samples, we estimate that the overall sensitivity gain with respect to a dry sample at room temperature[17] ($\Sigma^+ \approx 3.0\Sigma$) is between 10 and 30, corresponding to a reduction in experimental time by a factor between 100 and 900. This allows high quality one-dimensional ^{13}C CPMAS spectra of **1**–**3** to be acquired in less than 5 min at natural isotopic abundance. For comparison, a ^{1}H-^{13}C CPMAS spectrum of **1** at room temperature with a similar signal-to-noise ratio has been recorded in 2.3 h using standard instrumentation (Figure S5). However, it should be noted that the full width at half height (Λ) of the ^{13}C resonances of all DNP solid-state NMR spectra of **1** are around 2.8 ppm, while

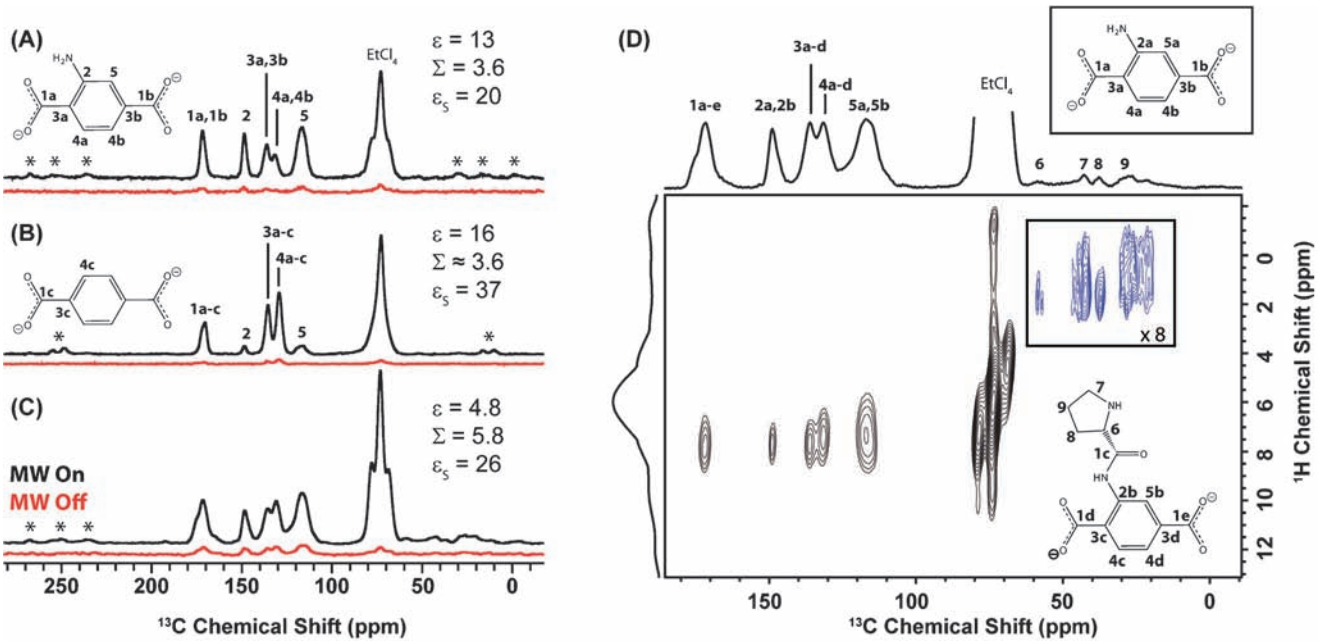

Figure 1. A–C) One-dimensional ^{1}H-^{13}C CPMAS spectra of **1**, **2** and **3**, respectively, recorded with (black) or without microwave irradiation (red) to induce DNP. The samples were impregnated with a 16 mM bTbK $EtCl_4$ solution. Both the observed (ε) and overall signal enhancement factors (Σ) provided by the DNP experiment are listed. DNP enhancement factors for the solvent resonance (ε_S) are also provided. All spectra were acquired on a Bruker 9.4 T DNP solid-state NMR spectrometer[9] equipped with an Avance III console and a low-temperature 3.2 mm triple resonance probe. In all cases the sample spinning frequency (ν_{rot}) was 12 kHz and sample temperatures were ca. 105 K. A total of 64 scans (A), or 128 scans (B and C) were accumulated with a CP contact time of 1 ms and a recycle delay of 1 s. Spinning sidebands are marked with asterisks. D) Two-dimensional ^{1}H-^{13}C HETCOR spectrum of **3**. A total of 512 scans were accumulated for each of the 72 t_1 increments ($\Delta t_1 = 67.20$ μs). A 1 s recycle delay and a 1 ms CP contact pulse were used (10.6 h total experiment time). During t_1 e-DUMBO-1_{22} ^{1}H decoupling[10] was applied at a radio-frequncy field strenght of 90 kHz. A scaling factor of 0.56 has been used to correct the proton chemical shift scale.

at room temperature Λ is 1.2 ppm (Figure S6) and is typical of a crystalline MOF.[3c,4] The increase in Λ primarily originates from the low sample temperatures and inclusion of the solvent in the pores of the material. Therefore, the DNP and Boltzmann signal enhancements are slightly offset by increases in Λ. Despite the slightly broader peaks, the DNP ^{13}C solid-state NMR spectra can readily be used to obtain structural information about the materials.

Assignment of the carbon resonances is reported in Figure 1, based on the chemical shift values and on comparison of the various spectra. Notably, the resonances corresponding to carbons 2 and 5 of the aminoterephthalate are clearly identified based on the fact that their intensity is reduced in Figure 1 B, as only 20 % of the linkers contained an amine moiety in **2**. The spectra of **3** are consistent with the replacement of 10 % of the amine functionalities with proline ligands. In the aliphatic region of the 1D ^{13}C CPMAS spectrum (Figure 1 C), the resonances from the carbon nuclei of proline are hardly visible and overlap with the spinning sidebands of the aromatic resonances. The corresponding correlations are, however, unambiguously observed in the 2D dipolar ^{1}H-^{13}C heteronuclear correlation (HETCOR) spectrum (Figure 1 D). With the signal enhancement afforded by low temperature DNP experiments the 2D HETCOR spectrum could be acquired in 10.6 h. Note that without DNP, the acquisition of a such a spectrum with high enough signal-to-noise ratio to observe the weak proline resonances would require experiment times on the order of weeks. It should also be noted that it was possible to acquire a 2D ^{1}H-^{13}C HETCOR spectrum of **1** in 22 min (Figure S7).

DNP-enhanced ^{1}H-^{15}N CPMAS solid-state NMR spectra of **1**–**3** are shown in Figure 2. Natural abundance ^{15}N solid-state NMR experiments represent a considerable challenge due to the low gyromagnetic ratio ($\nu_0 = 40.58$ MHz at 9.4 T) and low natural abundance (N.A. = 0.37 %) of ^{15}N. Grant and co-workers have previously employed DNP to acquire natural abundance ^{1}H-^{15}N CPMAS solid-state NMR spectra of carbazole at low field (1.4 T).[20] Under the DNP conditions developed here, a high-resolution 9.4 T ^{1}H-^{15}N CPMAS spectrum of **1** with a reasonable signal-to-noise ratio could be acquired within 34 min (for comparison, at room temperature and using standard NMR instrumentation, the acquisition of a spectrum of similar signal-to-noise ratio required 13 h, Figure S8). The ^{15}N CPMAS spectrum of **1** shows a single broad resonance at a chemical shift of 66 ppm, consistent with a neutral primary amine bound to an aromatic carbon (an aniline). The ^{15}N CPMAS spectrum of **2** required a longer experimental time (2.3 h) to attain a reasonable S/N, due to the reduction in the number of ^{15}N spins by a factor of 80 % in comparison to **1**. As expected, the ^{15}N resonance of **2** has a similar chemical shift as for **1**. The spectrum of **3** (recorded in 5 h) shows the presence of two additional ^{15}N resonances consistent with the incorporation of proline into the MOF material. The proline amine resonance is observed

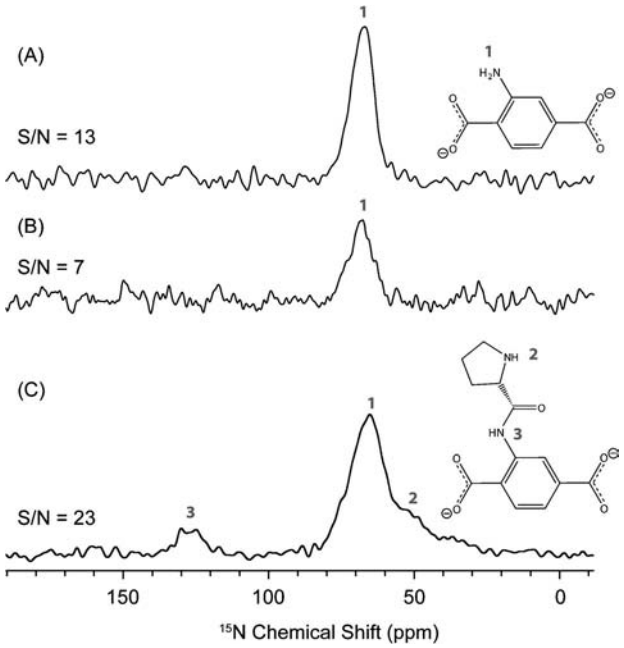

Figure 2. DNP ^{1}H-^{15}N CPMAS solid-state NMR spectra of **1**–**3**. All spectra were acquired with $\nu_{rot} = 12$ kHz and a 2.0 ms contact time. All spectra were processed with 50 Hz exponential line broadening. A) **1**, acquired with a 1 s recycle delay between each of 2048 scans (34 min total experiment time), B) **2**, acquired with a 2 s recycle delay between each of 4096 scans (2.3 h total experiment time), and C) **3**, acquired with a 1 s recycle delay between each of 18000 scans (5 h total experiment time). The signal-to-noise (S/N) ratios of the largest peaks are listed to the left of each spectrum. Chemical shifts are referenced to the NH_4^+ resonance ($\delta_{iso} = 0$ ppm) of ammonium nitrate.

as a shoulder ($\delta_{iso} = 50$ ppm) on the side of the aniline resonance while the amide resonance is centered at $\delta_{iso} =$ 127 ppm.

In summary, we have presented here the first application of DNP-enhanced solid-state NMR spectroscopy to MOFs. We have shown, on a series of three N-functionalized MOFs, that incipient wetness impregnation can readily be applied to impregnate these materials with radical-containing solution. DNP methodology provides reduction in experimental time of two orders of magnitude, even in the proline derivative material for which the radical does not enter into the pores. This enabled the fast acquisition of ^{13}C and ^{15}N NMR spectra with high S/N ratio. While the standard method used to characterize N-functionalized MOFs typically consists in the entire digestion/dissolution of the solids into strongly acidic solutions to enable solution NMR and mass spectrometry experiments,[16a,c,21] the strategy proposed here allows for the rapid characterization of intact MOF topologies. As such, DNP-enhanced solid-state NMR spectroscopy is expected to be applicable for the widespread characterization of MOFs.

Received: August 25, 2011
Published online: November 15, 2011

Keywords: dynamic nuclear polarization · hyperpolarization · metal–organic frameworks · solid-state NMR spectroscopy

[1] a) G. Férey, *Chem. Soc. Rev.* **2008**, *37*, 191 – 214; b) S. Kitagawa, R. Kitaura, S. Noro, *Angew. Chem.* **2004**, *116*, 2388 – 2430; *Angew. Chem. Int. Ed.* **2004**, *43*, 2334 – 2375; c) O. M. Yaghi, M. O'Keeffe, N. W. Ockwig, H. K. Chae, M. Eddaoudi, J. Kim, *Nature* **2003**, *423*, 705 – 714.

[2] B. F. Hoskins, R. Robson, *J. Am. Chem. Soc.* **1989**, *111*, 5962 – 5964.

[3] a) D. Farrusseng, S. Aguado, C. Pinel, *Angew. Chem.* **2009**, *121*, 7638 – 7649; *Angew. Chem. Int. Ed.* **2009**, *48*, 7502 – 7513; b) T. Loiseau, L. Lecroq, C. Volkringer, J. Marrot, G. Ferey, M. Haouas, F. Taulelle, S. Bourrelly, P. L. Llewellyn, M. Latroche, *J. Am. Chem. Soc.* **2006**, *128*, 10223 – 10230; c) C. Volkringer, D. Popov, T. Loiseau, N. Guillou, G. Ferey, M. Haouas, F. Taulelle, C. Mellot-Draznieks, M. Burghammer, C. Riekel, *Nat. Mater.* **2007**, *6*, 760 – 764.

[4] C. Volkringer, M. Meddouri, T. Loiseau, N. Guillou, J. Marrot, G. Ferey, M. Haouas, F. Taulelle, N. Audebrand, M. Latroche, *Inorg. Chem.* **2008**, *47*, 11892 – 11901.

[5] Y. Matsuki, T. Maly, O. Ouari, H. Karoui, F. Le Moigne, E. Rizzato, S. Lyubenova, J. Herzfeld, T. Prisner, P. Tordo, R. G. Griffin, *Angew. Chem.* **2009**, *121*, 5096 – 5100; *Angew. Chem. Int. Ed.* **2009**, *48*, 4996 – 5000.

[6] a) S. Horike, R. Matsuda, D. Tanaka, S. Matsubara, M. Mizuno, K. Endo, S. Kitagawa, *Angew. Chem.* **2006**, *118*, 7384 – 7388; *Angew. Chem. Int. Ed.* **2006**, *45*, 7226 – 7230; b) D. I. Kolokolov, H. Jobic, A. G. Stepanov, M. Plazanet, M. Zbiri, J. Ollivier, V. Guillerm, T. Devic, C. Serre, G. Ferey, *Eur. Phys. J. Spec. Top.* **2010**, *189*, 263 – 271; c) M. A. Springuel-Huet, A. Nossov, Z. Adem, F. Guenneau, C. Volkringer, T. Loiseau, G. Ferey, A. Gedeon, *J. Am. Chem. Soc.* **2010**, *132*, 11599 – 11607.

[7] a) R. G. Griffin, T. F. Prisner, *Phys. Chem. Chem. Phys.* **2010**, *12*, 5737 – 5740; b) T. Maly, G. T. Debelouchina, V. S. Bajaj, K. N. Hu, C. G. Joo, M. L. Mak-Jurkauskas, J. R. Sirigiri, P. C. A. van der Wel, J. Herzfeld, R. J. Temkin, R. G. Griffin, *J. Chem. Phys.* **2008**, *128*, 052211; c) T. Prisner, W. Kockenberger, *Appl. Magn. Reson.* **2008**, *34*, 213 – 218.

[8] A. Lesage, M. Lelli, D. Gajan, M. A. Caporini, V. Vitzthum, P. Mieville, J. Alauzun, A. Roussey, C. Thieuleux, A. Mehdi, G. Bodenhausen, C. Copéret, L. Emsley, *J. Am. Chem. Soc.* **2010**, *132*, 15459 – 15461.

[9] M. Rosay, L. Tometich, S. Pawsey, R. Bader, R. Schauwecker, M. Blank, P. M. Borchard, S. R. Cauffman, K. L. Felch, R. T. Weber, R. J. Temkin, R. G. Griffin, W. E. Maas, *Phys. Chem. Chem. Phys.* **2010**, *12*, 5850 – 5860.

[10] B. Elena, G. de Paepe, L. Emsley, *Chem. Phys. Lett.* **2004**, *398*, 532 – 538.

[11] M. Lelli, D. Gajan, A. Lesage, M. A. Caporini, V. Vitzthum, P. Mieville, F. Heroguel, F. Rascon, A. Roussey, C. Thieuleux, M. Boualleg, L. Veyre, G. Bodenhausen, C. Copéret, L. Emsley, *J. Am. Chem. Soc.* **2011**, *133*, 2104 – 2107.

[12] a) K. Barthelet, J. Marrot, G. Ferey, D. Riou, *Chem. Commun.* **2004**, 520 – 521; b) A. Fateeva, P. Horcajada, T. Devic, C. Serre, J. Marrot, J. M. Greneche, M. Morcrette, J. M. Tarascon, G. Maurin, G. Ferey, *Eur. J. Inorg. Chem.* **2010**, 3789 – 3794; c) M. Savonnet, D. Bazer-Bachi, N. Bats, J. Perez-Pellitero, E. Jeanneau, V. Lecocq, C. Pinel, D. Farrusseng, *J. Am. Chem. Soc.* **2010**, *132*, 4518 – 4519.

[13] M. Savonnet, D. Bazer-Bachi, C. Pinel, V. Lecocq, N. Bats, D. Farrusseng, FR Patent, 09/05.107, **2009**.

[14] J. Canivet, S. Aguado, G. Bergeret, D. Farrusseng, *Chem. Commun.* **2011**, *47*, 11650 – 11652.

[15] a) W. Kleist, F. Jutz, M. Maciejewski, A. Baiker, *Eur. J. Inorg. Chem.* **2009**, 3552 – 3561; b) W. Kleist, M. Maciejewski, A. Baiker, *Thermochim. Acta* **2010**, *499*, 71 – 78; c) S. Marx, W. Kleist, J. Huang, M. Maciejewski, A. Baiker, *Dalton Trans.* **2010**, *39*, 3795 – 3798.

[16] a) S. M. Cohen, *Chem. Sci.* **2010**, *1*, 32 – 36; b) K. K. Tanabe, S. M. Cohen, *Chem. Soc. Rev.* **2011**, *40*, 498 – 519; c) Z. Q. Wang, K. K. Tanabe, S. M. Cohen, *Inorg. Chem.* **2009**, *48*, 296 – 306.
[17] A. J. Rossini, A. Zagdoun, M. Lelli, D. Gajan, F. Rascon, M. Rosay, W. E. Maas, C. Copéret, A. Lesage, L. Emsley, *Chem. Sci.* **2011**, DOI: 10.1039/c1sc00550b.
[18] A. Zagdoun, A. J. Rossini, D. Gajan, A. Bourdolle, O. Ouari, M. Rosay, W. E. Maas, P. Tordo, M. Lelli, L. Emsley, A. Lesage, C. Copéret, *Chem. Commun.* **2011**, DOI: 10.1039/c1cc15242d.
[19] P. C. A. van der Wel, K. N. Hu, J. Lewandowski, R. G. Griffin, *J. Am. Chem. Soc.* **2006**, *128*, 10840 – 10846.
[20] J. Z. Hu, M. S. Solum, R. A. Wind, B. L. Nilsson, M. A. Peterson, R. J. Pugmire, D. M. Grant, *J. Phys. Chem. A* **2000**, *104*, 4413 – 4420.
[21] K. K. Tanabe, S. M. Cohen, *Angew. Chem.* **2009**, *121*, 7560 – 7563; *Angew. Chem. Int. Ed.* **2009**, *48*, 7424 – 7427.

